

Electronic Supplementary Information for

Strong p - d orbital hybridization on PdSn metallene for enhanced electrooxidation of plastic-derived alcohols to glycolic acid

Ziqiang Wang, Yanan Wang, Jiayao Chen, Hongjie Yu, You Xu, Kai Deng*,

Hongjing Wang* and Liang Wang*

Zhejiang Key Laboratory of Surface and Interface Science and Engineering for Catalysts, Zhejiang University of Technology, Hangzhou, Zhejiang 310014, P. R. China

Corresponding authors

E-mails: kaideng@zjut.edu.cn; hjw@zjut.edu.cn; wangliang@zjut.edu.cn

Materials and reagents

Palladium diacetylacetonate ($\text{Pd}(\text{acac})_2$), Tin acetylacetonate ($\text{C}_{10}\text{H}_{14}\text{O}_4\text{Sn}$), N,N-dimethylformamide (DMF, 99.5%), acetate ($\text{CH}_3\text{CO}_2\text{H}$, 99.5%), potassium hydroxide (KOH), ethanol ($\text{C}_2\text{H}_5\text{OH}$), ethylene glycol (EG) were purchased from Aladdin. Tungsten carbonyl ($\text{W}(\text{CO})_6$) was purchased from Macklin.

Characterization

Scanning electron microscopy (SEM, Zeiss Gemini 500) equipped with an energy dispersive X-ray spectroscopy (EDX) system was used to characterize the morphology and structure of the synthesized samples. A TalosS-FEG instrument was used for transmission electron microscopy (TEM), high-resolution TEM (HRTEM) and high-angle annular dark-field scanning TEM (HAADF-STEM) images. X-ray diffraction (XRD) patterns were recorded using a PANalytical X'Pert PRO powder diffractometer. Cu $K\alpha$ radiation ($\lambda = 0.1541 \text{ nm}$) was used. A Thermo Scientific K-Alpha instrument was used for X-ray photoelectron spectroscopy (XPS) analysis. Atomic force microscopy (AFM, Bruker Dimension Icon) was used for measurement of catalyst thickness (data support from Shiyanjia Lab (<https://www.Shiyanjia.com>)).

Quantification of glycolic acid

The electrochemically oxidized solution (0.5 mL) was mixed with a deuterium oxide (D_2O) solution (0.1 mL) containing 10 mg mL^{-1} maleic acid (internal standard) to quantitatively determine the concentration of glycolic acid in the electrolytic products. ^1H and ^{13}C NMR spectra of the mixed solution were obtained by NMR. In ^1H NMR, D_2O showed a peak value of $\sim 4.8 \text{ ppm}$, EG was $\sim 3.5 \text{ ppm}$, and maleic acid was $\sim 5.9 \text{ ppm}$. In addition, the peak of glycolic acid is $\sim 3.73 \text{ ppm}$, and the peak of formic acid is about $\sim 8.25 \text{ ppm}$.

The calculations of the Faradaic efficiency (FE)

$$FE = zFcV/Q \quad (1)$$

Where z is the electron transfer number, F is the Faraday constant (96485 C mol^{-1}), c is the measured GA concentrations, V is the electrolyte volume, and Q is the total charge during electrolysis.

Theoretical calculations

We utilized the Vienna ab initio simulation package (VASP) to perform density functional theory (DFT) calculations, utilizing projector augmented wave (PAW) potentials and setting a plane-wave cutoff energy at 520 eV.^{1,2} The exchange-correlation functional was employed by generalized gradient approximation (GGA) functional of Perdew, Burke, and Ernzerhof (PBE) with Grimme's semiempirical DFT-D3 dispersion correction to account for van der Waals (vdW) interactions.³ Energy and force convergence criteria for structure optimization were set to 10^{-5} eV and 0.02 eV \AA^{-1} , respectively. A bulk Pd model was constructed using the Fm-3m space group, followed by the creation of a four-layer supercell for the Pd (111) model, with the vacuum layer of 16 Å. Subsequently, a certain amount of Sn atoms was randomly replaced with Pd atoms to build the PdSn (111) model. The Gibbs free energy change (ΔG) was determined using the formula ($\Delta G = \Delta E + \Delta ZPE - T\Delta S$), where ΔE represented the difference of the adsorption energy, while ΔZPE and ΔS signify the changes of zero-point energy and entropy, respectively. The computational hydrogen electrode (CHE) model was used for the ΔG of the electrochemical reaction steps.⁴ The Crystal Orbital Hamilton Populations (COHP) calculations were carried out by the LOBSTER package.^{5,6} The VASPKIT code was employed for post-processing of the computational data, while the VESTA package was used for visualization of the crystal structure.^{7,8}

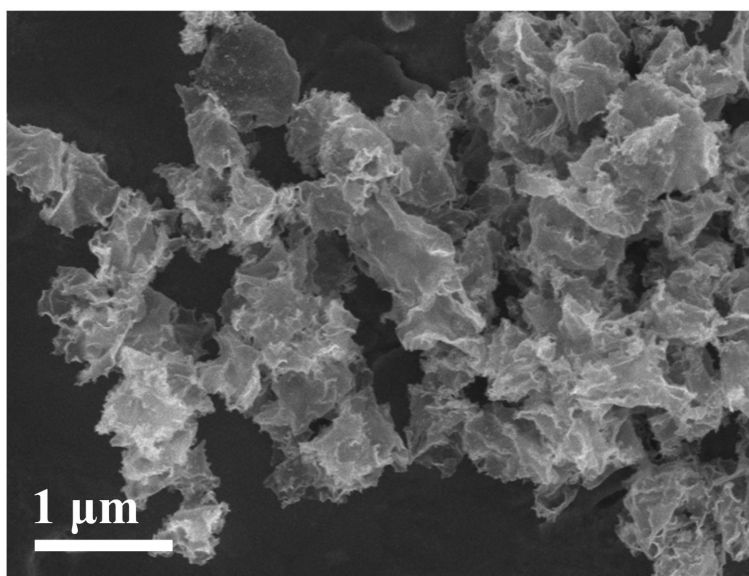


Fig. S1 SEM image of PdSn metallene.

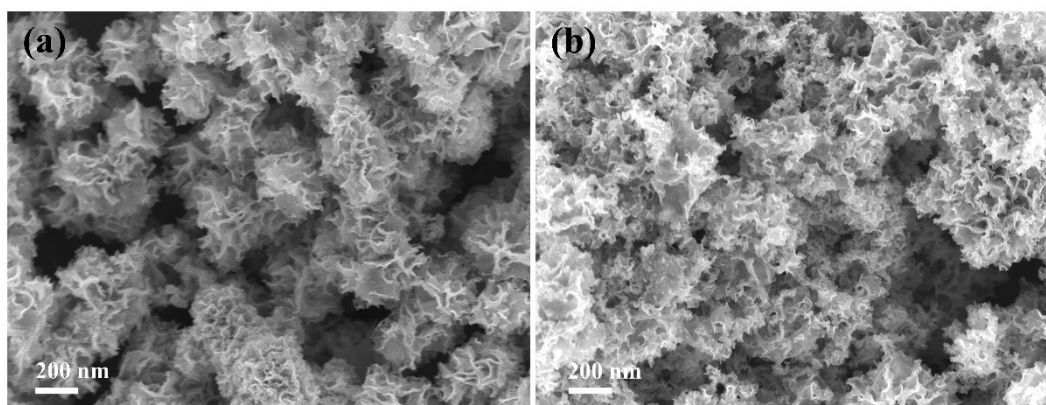


Fig. S2 SEM images of H-PdSn metallene (a) and L-PdSn metallene (b) with precursor mass ratios of 4:1 and 2:1, respectively.

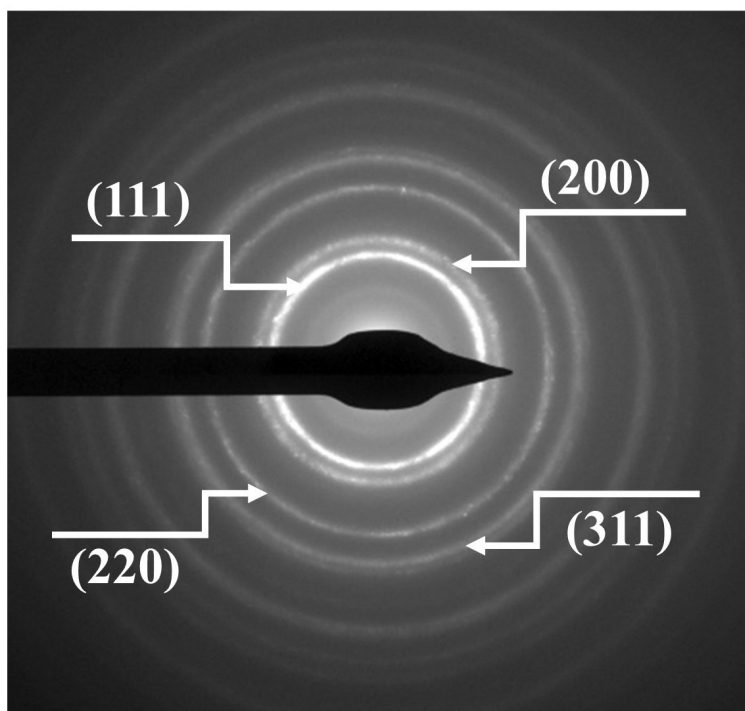


Fig. S3 SAED image of the PdSn metallene.

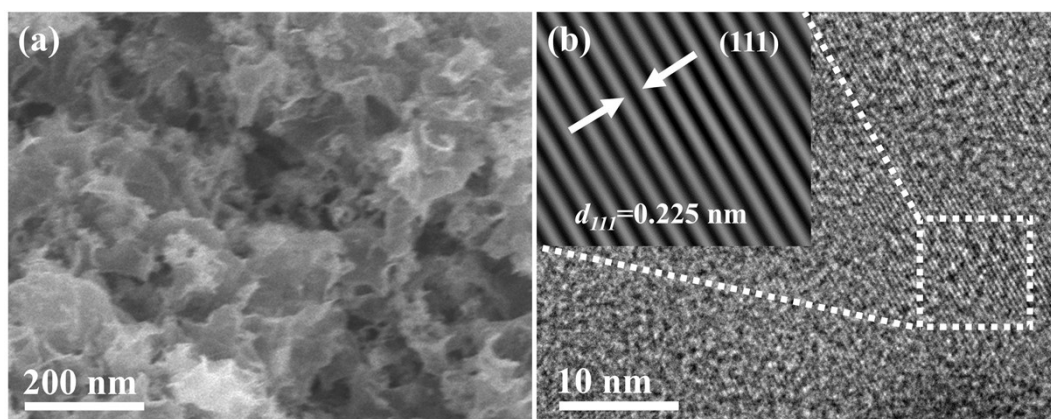


Fig. S4 (a) SEM and (b) HRTEM images of Pd metallene.

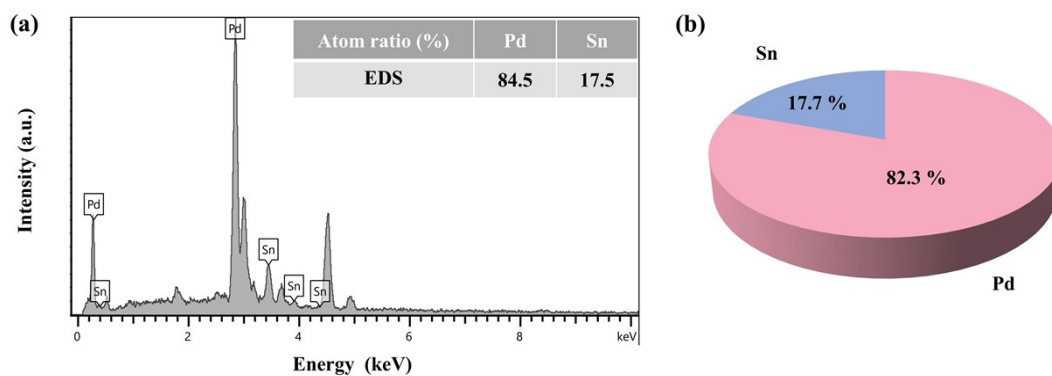


Fig. S5 (a) EDS and (b) ICP results of PdSn metallene.

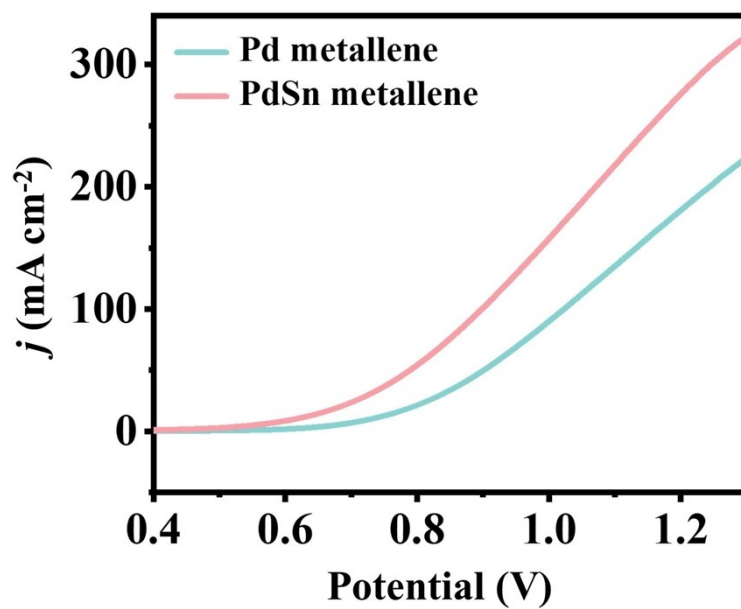


Fig. S6 LSV curves of Pd metallene and PdSn metallene in PET hydrolysate solution.

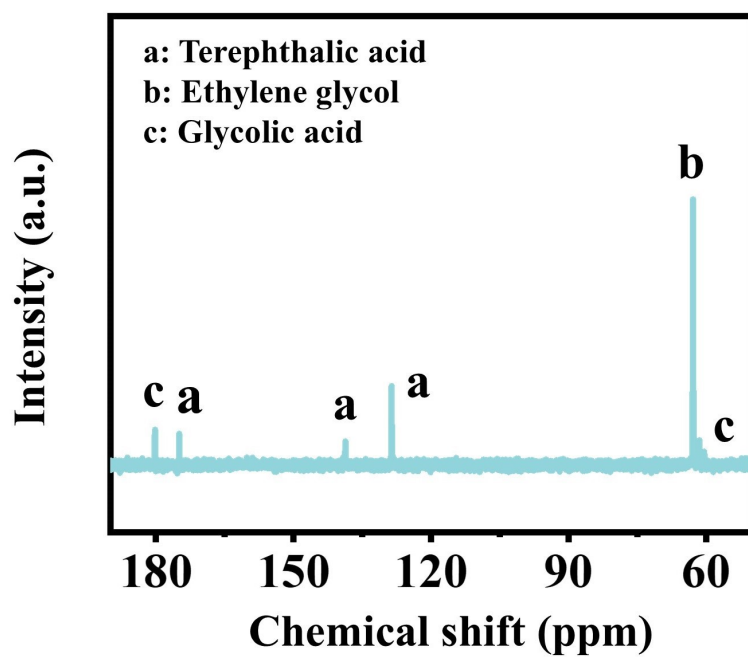


Fig. S7 ^{13}C NMR spectrum of electrolysis solution over PdSn metallene.

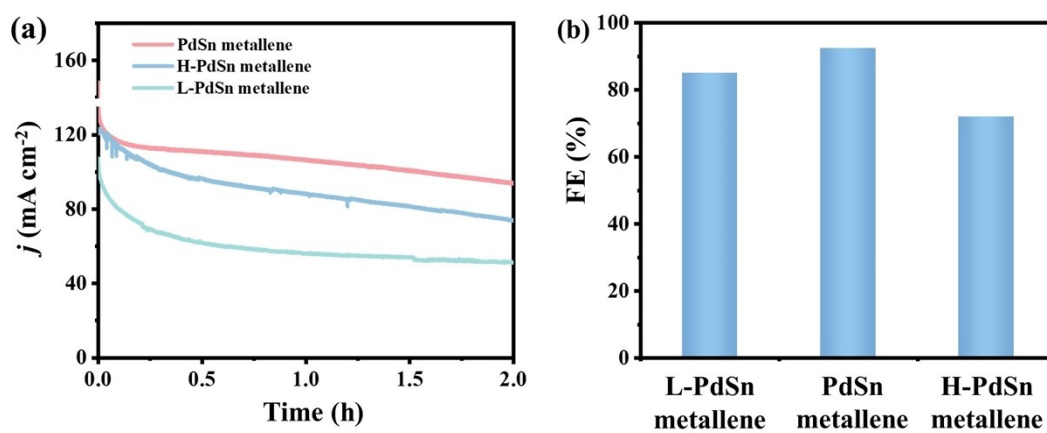


Fig. S8 The i-t curves under PET hydrolysate and FE values of samples with different precursor mass ratios for GA production.

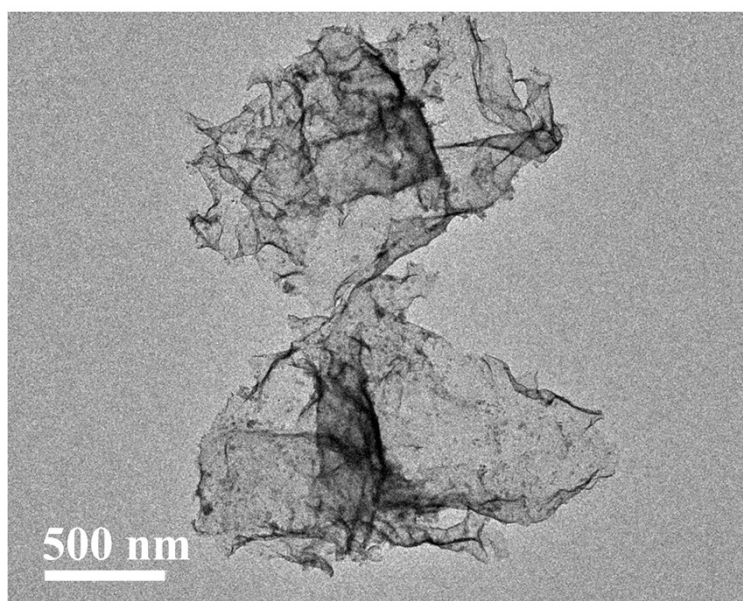


Fig. S9 TEM image of PdSn metallene after stability test.

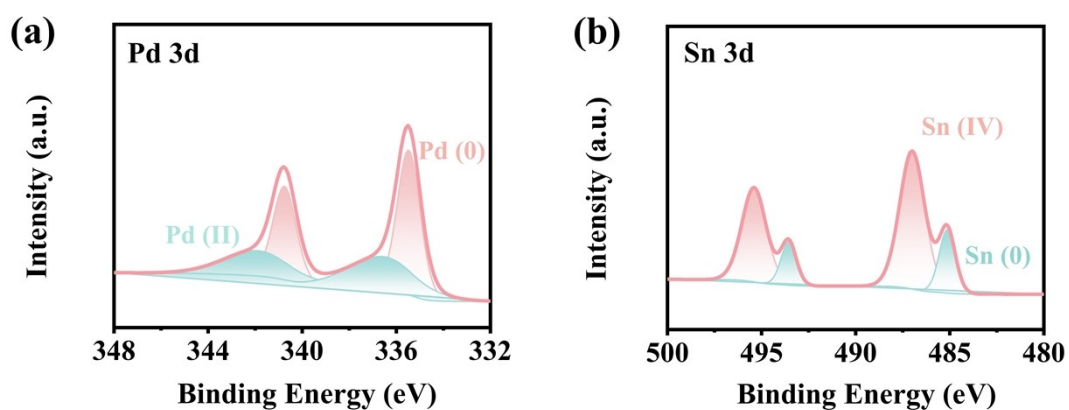


Fig. S10 XPS spectra of PdSn metallene after stability test.

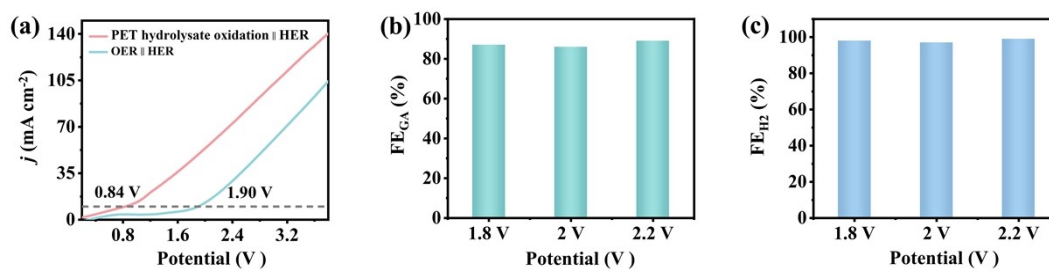


Fig. S11 (a) LSV curves of PdSn metallene in H-type cell. (b) FE_{GA} and (c) FE_{H₂} at various potentials.

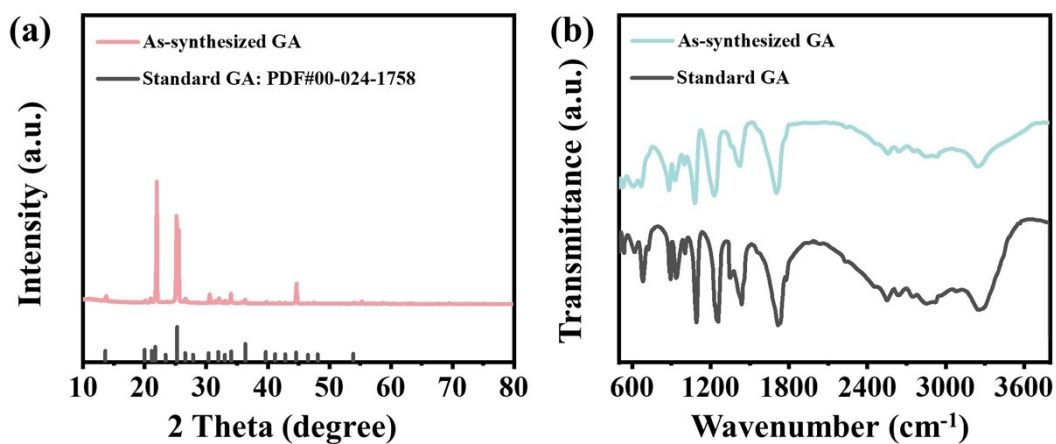


Fig. S12 (a) XRD pattern (b) Infrared spectrum of the recovered GA product.

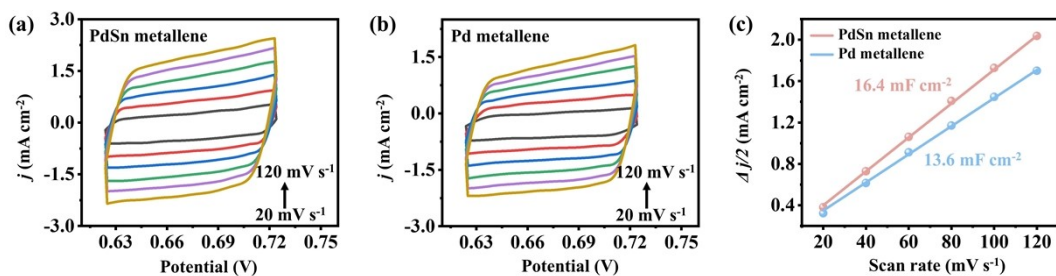


Fig. S13 CV curves of (a) PdSn metallene and (b) Pd metallene with various scan rates from 20 to 120 mV s⁻¹. (c) Plots of the current density versus the scan rate for PdSn metallene and Pd metallene.

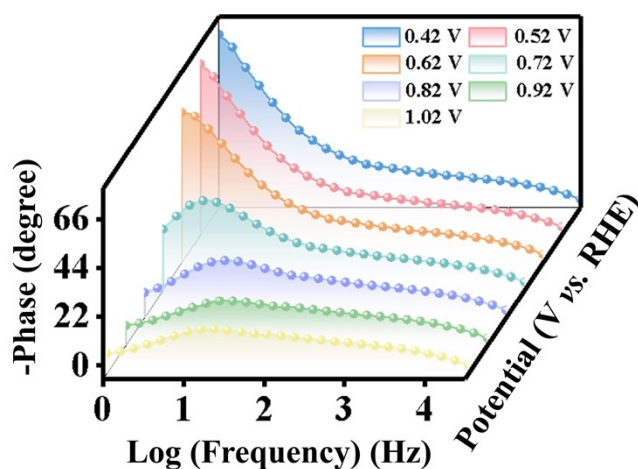


Fig. S14 Bode plots of Pd metallene in 1 M KOH and 1 M EGD electrolyte.

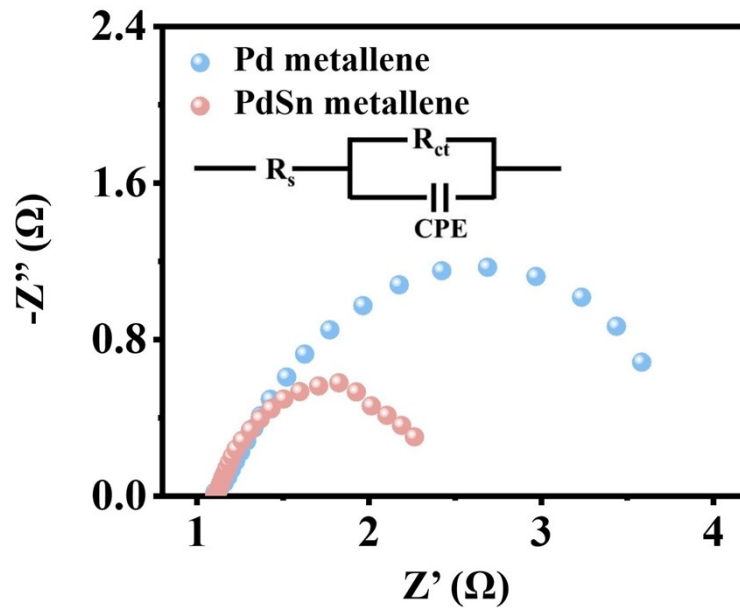


Fig. S15 EIS spectra of Pd metallene and PdSn metallene in 1 M KOH and 1 M EGD at 0.97 V.

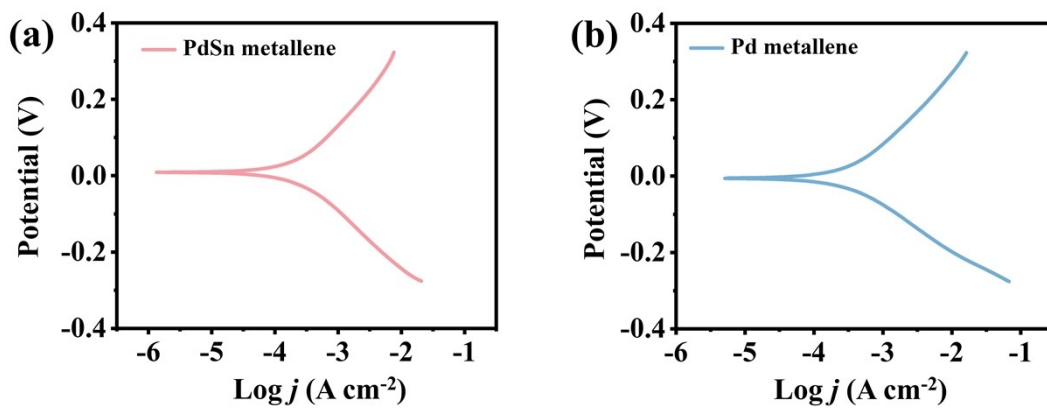


Fig. S16 Corrosion polarization curves of (a) PdSn metallene and (b) Pd metallene.

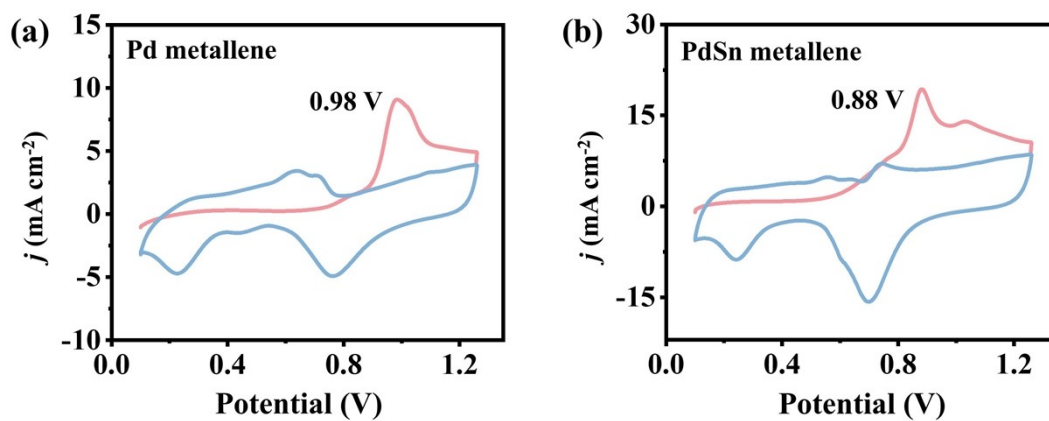


Fig. S17 CO stripping experiments of (a) Pd metallene and (b) PdSn metallene.

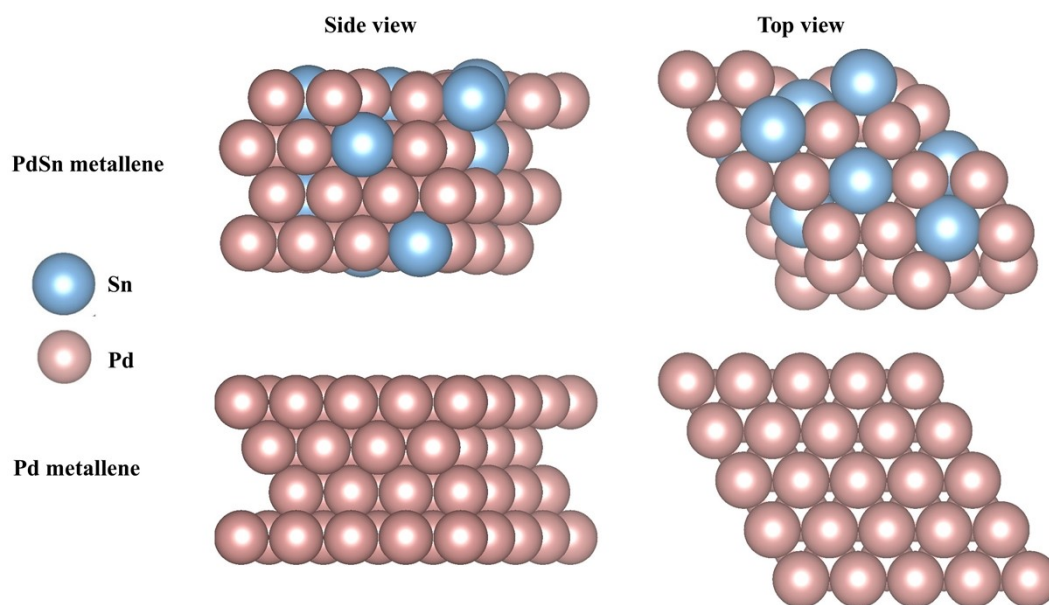


Fig. S18 Theoretical calculation models of PdSn and Pd.

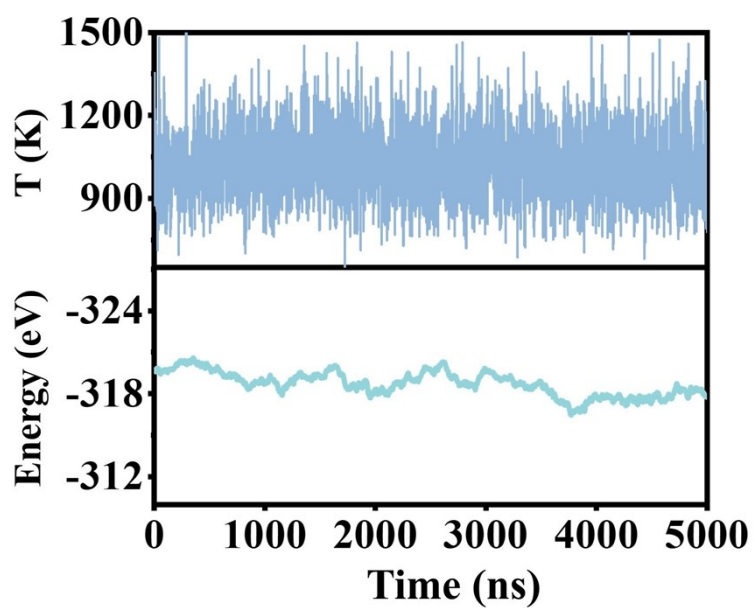


Fig. S19 Energy and temperature versus time during AIMD simulation for PdSn. The temperature was set to 1000 K.

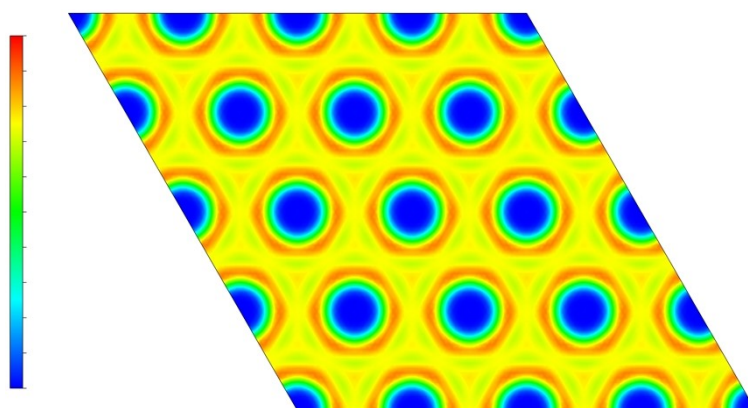


Fig. S20 Sliced ELF map of Pd along the (001) plane.

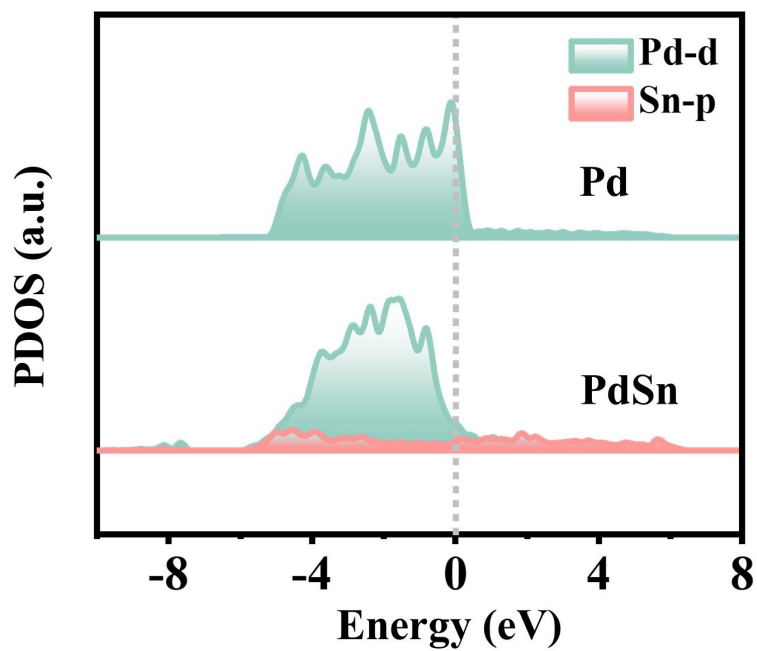


Fig. S21 PDOS profiles of Pd and PdSn.

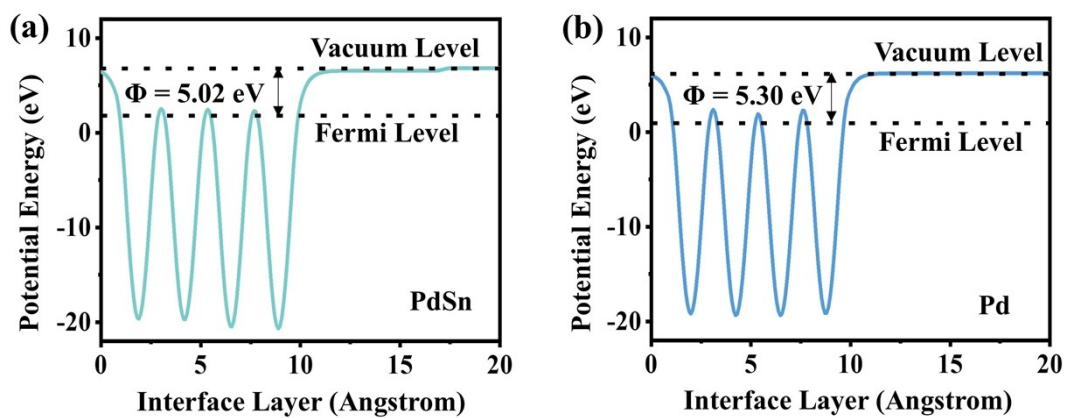


Fig. S22 Work function of (a) PdSn and (b) Pd.

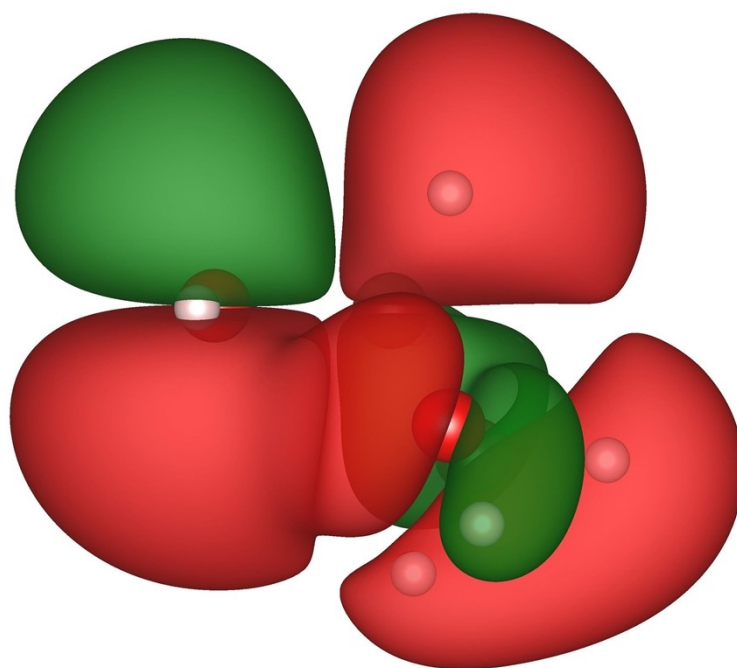


Fig. S23 The highest occupied molecular orbital of ethylene glycol.

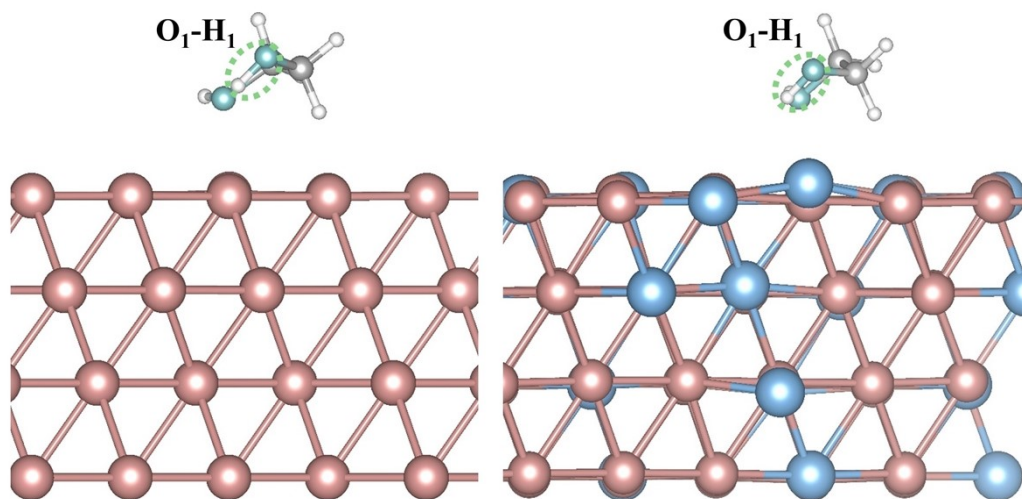


Fig. S24 The structure configurations of EG adsorbed Pd and PdSn models.

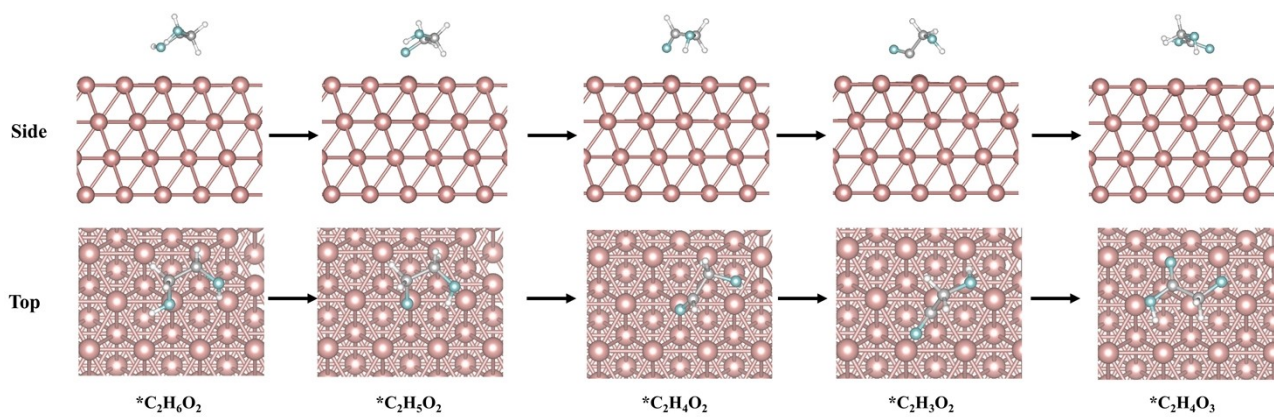


Fig. S25 The optimized configurations of EGOR intermediates adsorbed on Pd.

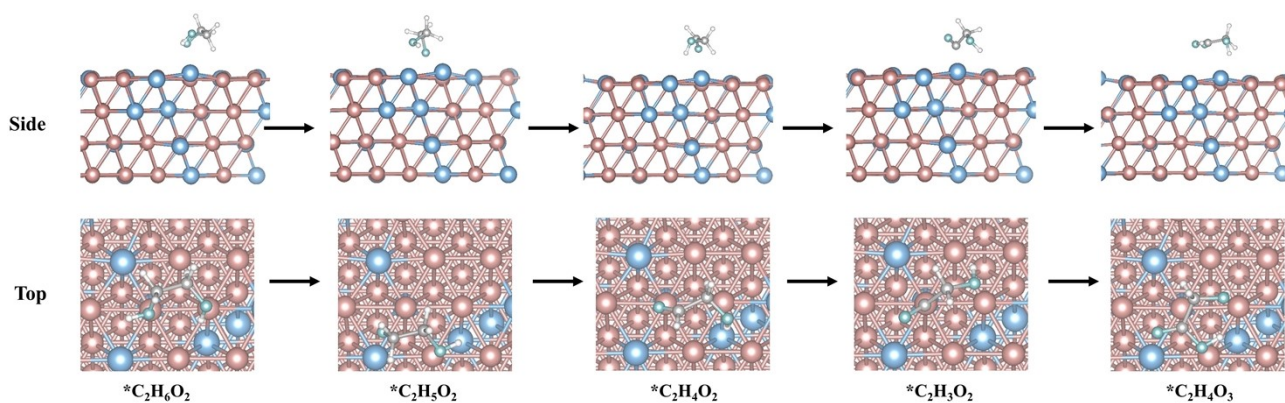


Fig. S26 The optimized configurations of EGOR intermediates adsorbed on PdSn.

Supplementary Note 1

To assess the economic feasibility of the coupling system, a Techno-economic Analysis (TEA) is conducted based on the Sargent Group model for the coupling reaction process. As an example, the analysis considers a daily production capacity of 1 ton of GA, with an anode current density of 55 mA cm⁻² and a FE of 86%. It is assumed that the FE for hydrogen production is 100%. The main assumptions used in the TEA are summarized below.

1. The electricity price is assumed to be 0.1 \$/kWh. The electricity expenses are categorized into three primary components: the electrolyzer for processing PET hydrolysate, the hydrolyzer for PET depolymerization, and the separation units for distillation and drying. It is assumed that the energy consumption for hydrolysis and product separation is the same as that of the electrolysis process.
2. The electrolyzer cost was assume of 10000 \$ per m².
3. The expected lifespan of the electrolyzer is 30 years, with a capacity factor of 0.8, indicating that the plant will operate for 19.2 hours each day.
4. The cost of the catalyst and membrane together accounts for 5% of the total electrolyzer cost.
5. The electrolyte cost is defined as 30% of the cost of the solid raw material.
6. It is assumed that the operation and maintenance costs are 10% of the capital costs.
7. The separation cost is assumed to be 30% of the total electricity cost.
8. It is assumed that the overall yield for converting PET to EG and its subsequent oxidation to GA is 50%, with a TPA yield of 85% and an impurity level of 10% in the PET feedstock.

The calculation process:

Capital cost

- 1) Electrolyzer cost:

Electrolyzer cost per ton GA = Electrolyzer area m² × 10000 \$

$$Q = \frac{n(GA) \times z \times F}{FE} = \frac{1.31 \times 10^4 \text{ mol} \times 4 e^- \times 96485 \text{ C/mol}}{85\%} = 5.9 \times 10^9 \text{ C}$$

$$I = \frac{Q}{\text{daily operation time of power plant} \times \text{capacity factor}} = \frac{5.9 \times 10^9 \text{ C}}{24 \text{ h} \times 3600 \text{ s} \times 0.8} = 8.5 \times 10^4 \text{ A}$$

A

$$\text{Electrolyzer cost per ton GA} = \frac{8.5 \times 10^4 \text{ A}}{0.055 \text{ A cm}^{-2}} = 1.5 \times 10^6 \text{ \$}$$

2) Catalyst and membrane costs:

$$\text{Catalyst and membrane} = \text{Electrolyzer cost} \times 5\% = 1.5 \times 10^6 \times 5\% = 7.7 \times 10^4 \text{ \$}$$

$$\text{Capital cost} = \frac{\text{Electrolyzer cost} + \text{Catalyst and membrane}}{\text{Lifetime of plant}} = \frac{1.5 \times 10^6 \text{ \$} + 7.7 \times 10^4 \text{ \$}}{30 \text{ years} \times 365 \text{ day}} = 148.29 \text{ \$}$$

1. Maintenance cost:

$$\text{Maintenance cost} = \text{Capital cost} \times 10\% = 148.29 \text{ \$} \times 10\% = 14.83 \text{ \$}$$

2. Balance of plant:

$$\text{Balance of plant} = \text{Capital cost} \times \text{Balance of plant factor} = 148.29 \text{ \$} \times 0.35 = 51.90 \text{ \$}$$

3. Installation cost :

$$\text{Installation cost} = \text{Capital cost} \times \text{Lang factor} = 148.29 \text{ \$} \times 0.2 = 29.66 \text{ \$}$$

4. Electricity cost :

$$\text{Power} = \frac{I \times U}{10^3} \text{ KW} = \frac{8.5 \times 10^4 \text{ A} \times 1.8 \text{ V}}{10^3} = 153 \text{ KW}$$

$$\text{Energy use per day (kWh)} = \text{Power} \times \text{Time in a day(h)} \times \text{capacity}$$

$$= 153 \text{ KW} \times 24 \text{ h} \times 0.8 = 2939 \text{ kWh}$$

$$\text{Electricity cost of per day} = \text{Energy use per day} \times \text{Cost per kWh} = 2939 \times 0.1 \text{ \$} = 293.9 \text{ \$}$$

$$\text{Electricity costs per day} = 293.9 \text{ \$} \times 2 = 587.8 \text{ \$}$$

5. Separation cost:

$$\text{Separation cost} = \text{Electricity cost} \times 30\% = 587.8 \$ \times 30\% = 176.34 \$$$

6. Operating cost:

$$\text{Operating cost} = \text{Capital cost} \times 10\% = 148.29 \$ \times 10\% = 14.83 \$$$

7. Input chemicals cost : Materials require 2.22 ton of PET, 2 ton KOH, 1.74 ton H₂SO₄, and 4.44 ton water.

$$\text{Input chemicals cost} = 2.22 \text{ ton PET } (2.22 \times 390) + 2 \text{ ton KOH } (2 \times 1280) + 1.74 \text{ ton H}_2\text{SO}_4 (1.74 \times 45) + 4.44 \text{ ton water } (4.44 \times 0.22) = 3505 \$$$

8. Total cost:

$$\begin{aligned} \text{Total cost} &= \text{Capital cost} + \text{Maintenance cost} + \text{Balance of plant} + \text{Installation cost} + \text{Electricity cost} \\ &+ \text{Separation cost} + \text{Operating cost} + \text{Input chemicals cost} = 4528.65 \$ \end{aligned}$$

9. The products of this process include 1.7 ton TPA, 1 ton GA and 0.055 ton H₂.

$$\begin{aligned} \text{Total profit} &= 1.7 \text{ ton TPA } (1.7 \times 1260) + 1 \text{ ton GA } (1 \times 3100) + 0.055 \text{ ton H}_2 (0.061 \times 1900) = 5357.9 \\ &\$ \end{aligned}$$

$$10. \text{Gross Profit} = \text{Total profit} - \text{Total cost} = 5357.9 \$ - 4528.65 \$ = 829.25 \$$$

Table S1. Recent reports on ethylene glycol oxidation catalysts for high value-added product.

Catalyst	electrolyte	performance	products	Reference
PdSn metallene	PET hydrolysate	FE_{GA}: 92.45% (0.97 V vs. RHE)	GA	This work
PdAg/NF	1 M KOH + 1 M EG	FE _{GA} : 92% (0.91 V vs. RHE)	GA	9
Au/Ni(OH) ₂	3 M KOH + 0.3 M EG	FE _{GA} : 91% (1.15 V vs. RHE)	GA	10
Pd NTs/NF	PET hydrolysate	FE _{GA} : 87.87% (0.774 V vs. RHE)	GA	11
Pd-Ni(OH) ₂ /NF	1 M KOH + 1 M EG	FE _{GA} : 94.1% (1.0 V vs. RHE)	GA	12
CoNi _{0.25} P/NF	1 M KOH + 0.3 M EG	FE _{FA} : 91.7% (1.7 V vs. RHE)	FA	13
CuCo ₂ O ₄ NWA/NF	PET hydrolysate	FE _{FA} : 93% (1.5 V vs. RHE)	FA	14
Pd-NiTe/NF	PET hydrolysate	FE _{FA} : 96.5% (1.38 V vs. RHE)	FA	15
NiCo ₂ O ₄	PET hydrolysate	FE _{FA} : >90%	FA	16
Ni ₃ N/W ₅ N ₄	PET hydrolysate	FE _{FA} : 85%	FA	17

References

- 1 G. Kresse and J. Furthmüller, *Comput. Mater. Sci*, 1996, **6**, 15-50.
- 2 G. Kresse and J. Hafner, *Phys. Rev. B*, 1993, **47**, 558.
- 3 J. P. Perdew, K. Burke and M. Ernzerhof, *Phys. Rev. Lett.*, 1996, **77**, 3865.
- 4 J. K. Nørskov, J. Rossmeisl, A. Logadottir, L. Lindqvist, J. R. Kitchin, T. Bligaard and H. Jonsson, *J. Phys. Chem. B*, 2004, **108**, 17886-17892.
- 5 V. L. Deringer, A. L. Tchougréeff and R. Dronskowski, *J. Phys. Chem. A*, 2011, **115**, 5461-5466.
- 6 S. Maintz, V. L. Deringer, A. L. Tchougréeff and R. Dronskowski, *J. Comput. Chem.*, 2013, **34**, 2557-2567.
- 7 V. Wang, N. Xu, J. C. Liu, G. Tang and W.-T. Geng, *Comput. Phys. Commun.*, 2021, **267**, 108033.
- 8 K. Momma and F. Izumi, *J. Appl. Crystallogr.*, 2011, **44**, 1272-1276.
- 9 D. Si, B. Xiong, L. Chen and J. Shi, *Chem Catal.*, 2021, **1**, 941-955.
- 10 Y. Yan, H. Zhou, S.-M. Xu, J. Yang, P. Hao, X. Cai, Y. Ren, M. Xu, X. Kong and M. Shao, *J. Am. Chem. Soc.*, 2023, **145**, 6144-6155.
- 11 T. Ren, Z. Duan, H. Wang, H. Yu, K. Deng, Z. Wang, H. Wang, L. Wang and Y. Xu, *ACS Catal.*, 2023, **13**, 10394-10404.
- 12 F. Liu, X. Gao, R. Shi, Z. Guo, E. C. Tse and Y. Chen, *Angew. Chem., Int. Ed.*, 2023, **62**, e202300094.
- 13 H. Zhou, Y. Ren, Z. Li, M. Xu, Y. Wang, R. Ge, X. Kong, L. Zheng and H. Duan, *Nat. Commun.*, 2021, **12**, 4679.
- 14 F. Liu, X. Gao, R. Shi, C. Edmund and Y. Chen, *Green Chem.*, 2022, **24**, 6571-6577.
- 15 H. Zhang, Y. Wang, X. Li, K. Deng, H. Yu, Y. Xu, H. Wang, Z. Wang and L. Wang, *Appl.*

Catal., B, 2024, **340**, 123236.

16 J. Wang, X. Li, M. Wang, T. Zhang, X. Chai, J. Lu, T. Wang, Y. Zhao and D. Ma, *ACS Catal.*, 2022, **12**, 6722-6728.

17 F. Ma, S. Wang, X. Gong, X. Liu, Z. Wang, P. Wang, Y. Liu, H. Cheng, Y. Dai, Z. Zheng and B. Huang, *Appl. Catal., B*, 2022, **307**, 121198.